ARTICLE

Red-Green Color Vision Impairment in Duchenne Muscular Dystrophy

Marcelo Fernandes Costa, Andre Gustavo Fernandes Oliveira, Claudia Feitosa-Santana, Mayana Zatz, and Dora Fix Ventura

The present study evaluated the color vision of 44 patients with Duchenne muscular dystrophy (DMD) (mean age 14.8 years; SD 4.9) who were submitted to a battery of four different color tests: Cambridge Colour Test (CCT), Neitz Anomaloscope, Ishihara, and American Optical Hardy-Rand-Rittler (AO H-R-R). Patients were divided into two groups according to the region of deletion in the dystrophin gene: upstream of exon 30 ($n = 12$) and downstream of exon 30 ($n = 32$). The control group was composed of 70 age-matched healthy male subjects with no ophthalmological complaints. Of the patients with DMD, 47% (21/44) had a red-green color vision defect in the CCT, confirmed by the Neitz Anomaloscope with statistical agreement ($P < .001$). The Ishihara and the AO H-R-R had a lower capacity to detect color defects—5% and 7%, respectively, with no statistical similarity between the results of these two tests nor between CCT and Anomaloscope results ($P > .05$). Of the patients with deletion downstream of exon 30, 66% had a red-green color defect. No color defect was found in the patients with deletion upstream of exon 30. A negative correlation between the color thresholds and age was found for the controls and patients with DMD, suggesting a nonprogressive color defect. The percentage (66%) of patients with a red-green defect was significantly higher than the expected <10% for the normal male population ($P < .001$). In contrast, patients with DMD with deletion upstream of exon 30 had normal color vision. This color defect might be partially explained by a retina impairment related to dystrophin isoform Dp260.

Duchenne muscular dystrophy (DMD [MIM 310200]), which affects 1:3,500 newborn males,[1–3] is the most common form of progressive muscular dystrophy disease. It is caused by a deficiency in the protein called "dystrophin."[4] The dystrophin gene, at Xp21, has 79 exons.[2] DMD is caused by deletions in the dystrophin gene in 60%–65% of patients, by duplications in 5%–10%, and by point mutations or small rearrangements in the remaining 20%–30%. The main pathological effects caused by mutations in the dystrophin gene are in the skeletal and cardiac muscles, although dystrophin is present in several other tissues of the body, including a widespread distribution in the nervous system.[5]

In addition to full-length dystrophin, four other shorter proteins are transcribed from the DMD gene: Dp260 (transcripts spliced to exon 30), Dp140 (transcripts spliced to exon 44), Dp116 (transcripts spliced to exon 56), and Dp71 (transcripts spliced to exon 63).[6,7]

In the retina, dystrophin is expressed at the level of the outer plexiform layer (Dp260) in the inner limiting membrane (Dp71).[7–12] Dp260 is also found at the cone pedicle, in the region of the ribbon synapse.[13] Electrophysiological studies showed that Dp260 is essential for the physiology of the retina, since patients with DMD and deletions downstream of exon 30 had serious impairment in both scotopic and photopic responses obtained by full-field electroretinogram (ERG).[6,14–24] The role of Dp71 in the retinal electrophysiology is still unknown. In the work of Claudepierre et al.,[8] it was associated with the b-wave Muller cells' contribution to the ERG. Dp427 and Dp140 are also present in mouse retina but do not appear to make an important contribution to the ERG.[25]

Previous studies of color vision in patients with DMD or Becker muscular dystrophy (BMD), based on Ishihara and American Optical Hardy-Rand-Rittler (AO H-R-R) tests, found that the proportion of red-green defect in this group[26,27] was in accordance with the proportion observed for the normal population. However, the Ishihara and AO H-R-R tests are screening tests used to detect severe red-green deficiency,[28,29] but they are not sufficiently sensitive to detect moderate or light impairment. Recent studies have demonstrated an advantage of computerized color vision tests over the semiquantitative tests classically used in the evaluation of color vision, such as the Farnsworth-Munsell 100-Hue Test. The advantage is due to several aspects inherent to the programmed presentation of testing trials and to the advances in computerized color reproduction, since (1) rigorous psychophysical methodology is used, (2) changes in the chromatic steps can be varied according to the subject being tested, (3) the resolution of the chromatic steps is sufficiently fine to allow threshold measurement, and (4) online computation of

From the Laboratório da Visão, Departamento de Psicologia Experimental, Instituto de Psicologia, Universidade de São Paulo, and Núcleo de Neurociências e Comportamento, Universidade de São Paulo (M.F.C.; A.G.F.O.; C.F.-S.; D.F.V.), and Centro de Estudos do Genoma Humano, Instituto de Biociências Universidade de São Paulo (M.Z.), São Paulo, Brasil

Received February 1, 2007; accepted for publication March 15, 2007; electronically published April 13, 2007.

Address for correspondence and reprints: Dr. Marcelo Fernandes Costa, Universidade de São Paulo, Instituto de Psicologia, Departamento Psicologia Experimental, Avenida Prof. Mello Moraes, 1721, CEP 05508-900, São Paulo, SP, Brasil. E-mail: costamf@usp.br

Am. J. Hum. Genet. 2007;80:1064–1075. 0002-9297/2007/8006-0007$15.00
DOI: 10.1086/518127

the results is available. A shortcoming of the computerized tests is that they are new and experimental, and most are not commercially available. An exception to this limitation is a test designed by Mollon and Reffin,[30] which is available commercially as the Cambridge Colour Test (CCT).

In the present study, we therefore reexamined color vision in patients with DMD, using this new color vision test, which is much more detailed and has been rated as more sensitive than the traditional tests.[31–35] Because it is programmed to simultaneously test the three cone-isolation axes, the CCT allows a more refined analysis of the visual pathways involved in chromatic processing—the parvocellular pathway, which mediates red-green color vision, and the koniocellular pathway, which mediates yellow-blue color vision.[31,32,34,35] We also used the Anomaloscope test—a gold standard for the detection of red-green defect—and, in addition, the Ishihara and AO H-R-R tests, which had been used in the early studies of patients with DMD.

Methods

Subjects

We evaluated 50 patients with DMD ranging in age from 9 to 21 years (mean 14.9 years; SD 4.3) who were referred by the Associação Brasileira de Distrofia Muscular (ABDIM) and had been given diagnoses and been followed up by the Human Genome Research Center of the Institute of Biosciences of the University of São Paulo. This study followed the tenets of the Declaration of Helsinki. Informed consent was obtained from the subjects after the nature of the study was explained.

The diagnosis of DMD was established by clinical and neurological examination, family history, grossly elevated serum creatinine levels, and DNA analysis. It is known that ~60%–65% of patients with DMD have deletions in the dystrophin gene. Deletion screening used a set of 18 primers that allowed detection of 98% of the deleted exons and that were developed by Chamberlain[36] and Beggs.[37] Motor performance of the patients with DMD was assessed and classified according the Vignos Scale, a scale of motor-function evaluation specific to neuromuscular diseases.[38] The assessment was made by physiotherapists from the ABDIM staff. A total of 50 patients with known deletions in the dystrophin gene were selected for this study. They were classified into two groups according to the deleted region: patients with deletions upstream of exon 30 ($n = 12$) and patients with deletions downstream of exon 30 ($n = 38$). This distinction was made because retinal dystrophin, Dp260, is known to splice in at exon 30. The demographic data of the 50 patients with DMD are shown in table 1.

An ophthalmological examination was performed for all subjects, to eliminate confounding pathologies, such as cataracts, retinopathy, or neuropathy. Fundoscopy was performed with indirect ophthalmoscopy. Visual acuity was measured at 3 m with use of an ETDRS chart (tumbling E). All patients had normal eye fundus and 20/20 or better best-corrected visual acuity. To constitute the control group, 75 healthy male subjects ranging in age from 9 to 22 years (mean 13.9 years; SD 4.3) were tested. Inclusion criteria for this group were normal eye fundus, 20/20 or better best-corrected visual acuity, and absence of color vision defects. Five (7%) male subjects did not meet the criteria, since they had congenital color vision defect, and were excluded from the analysis. With these exclusions, the control group was composed of 70 subjects ranging in age from 9 to 22 years (mean 14.6 years; SD 4.9).

Equipment and Procedures

The evaluation of the color discrimination was performed using the commercial version of CCT (v2.0 [Cambridge Research Instruments]) installed in a personal computer (Dell Dimension XTC-600) with a graphic board VSG 2/5 (Cambridge Research Instruments). The stimuli were generated in a high-resolution color monitor, Sony FD Trinitron model GDM-F500T9 (Sony). Testing was conducted in a dark room with the patients positioned 3 m away from the monitor.

The stimulus provided by the CCT was similar to those used in the pseudoisochromatic plate tests, such as the Ishihara test (Kanehara & Co.) or the AO H-R-R (Richmond Products). The target consisted of a Landolt "C" that differed in chromaticity from the single neutral background (coordinates 0.1977, 0.4689 of $u'v'$ of the International Commission on Illumination [CIE] 1976 color space) (fig. 1). The Landolt C gap size corresponded to 1.25° of visual angle, with the outer diameter 5.4° and the inner diameter 2.75° at the test distance of 3 m. Both target and background were composed of small patches of varying sizes (0.5–2 cm in diameter) and six luminance levels (8, 10, 12, 14, 16, and 18 candela [cd] × m^{-2}) randomly distributed in the display. This design used spatial and luminance noise to avoid the influence of cues derived from luminance differences or from target contours in the intended hue discrimination.

The target was randomly presented with its opening in one of four positions: up, bottom, right, and left (4-Alternative Forced Choice strategy). The patient's task was to press one of the four buttons of the response box (CT3 [Cambridge Research Instruments]), to indicate the position of the "C" opening. The patients had up to 15 s to give the response. Patients with motor impairment verbally indicated the gap position, and the examiner pressed the buttons.

A psychophysical staircase procedure was used for threshold determination. Each staircase began with a saturated chromaticity, which was changed along the vector connecting it to the background chromaticity. The change depended on the patient's response: the target chromaticity approached the background chromaticity every time there was a correct response and moved away from it every time there was an incorrect response or no response. The chromaticity excursion along the vectors ranged from 0.1100 to 0.0020 units of CIE 1976 $u'v'$. After six staircase reversals, the program automatically calculated the threshold for that vector as the average of the chromaticities corresponding to the reversals. The step size used in the staircase followed a dynamic rule (for more details on the CCT methodology, see the work of Regan et al.,[39] and, for CCT norms, see the work of Ventura et al.[32]).

The CCT has two testing procedures. The Trivector test is used to determine thresholds along the protan, deutan, and tritan confusion lines (fig. 1). In this procedure, the three corresponding staircases are conducted simultaneously, in an interleaved way, changing randomly from one to the other. Periodically, a control target at maximum saturation is presented, as a catch trial.

The other CCT procedure is used for the construction of a discrimination ellipse (MacAdam ellipse). In this study, we used

Table 1. Demographic Data and Color Test Results for the Patients with DMD

Patient	Age	Deletion in Exon	CCT Trivector			CCT Ellipses		T/P	T/D	Neitz	Ishihara	H-R-R	Vignos
			Protan	Deutan	Tritan	Area	Angle						
1	21	8	56	69	109	437.2	75.0	1.9	1.6	N	N	N	…
2	20	7	49	62	88	608.4	60.3	1.8	1.4	N	N	N	9
3	10	5–13	97	98	130	793.7	178.7	1.3	1.3	N	N	N	8
4	17	8–27	39	35	58	169.8	67.6	1.5	1.7	…	…	…	8
5	17	8–9	46	46	75	569.7	72.6	1.6	1.6	…	N	N	9
6	23	3–7	176	470	64	10,000.0	159.6	.4	.1	D	D	D	7
7	10	11–15	69	54	97	587.1	70.1	1.4	1.8	N	N	N	6
8	15	8–12	58	62	59	509.8	68.3	1.02	.95	N	N	N	6
9	18	19	48	56	92	336.2	50.2	1.92	1.64	N	N	N	7
10	9	8–13	137	144	141	1,279.4	61.4	1.03	.98	N	N	N	4
11	11	8–13	119	102	113	765.8	41.3	.95	1.11	N	N	N	6
12	10	8–13	86	56	127	626.9	53.0	1.5	2.3	N	N	N	7
13	9	47–52	99	105	209	4,441.1	23.0	2.1	2.0	P	N	N	7
14	9	48–52	141	134	118	1,251.5	46.8	.8	.9	…	N	RG	7
15	15	50	88	89	110	881.2	52.1	1.3	1.2	N	N	N	…
16	15	47–48	69	79	117	708.8	57.7	1.7	1.5	…	N	N	9
17	12	50	81	64	81	478.5	105.5	1.0	1.3	N	N	N	9
18	20	40–42	…	…	…	…	…	…	…	…	…	…	7
19	12	50	156	174	149	1,498.9	145.7	1.0	.9	…	N	N	9
20	13	47–50	117	120	205	3,365.9	81.6	1.8	1.7	…	N	N	7
21	8	50	119	107	82	1,264.7	67.3	.7	.8	N	N	N	7
22	9	45	102	74	122	955.1	62.9	1.2	1.6	P	N	N	7
23	16	49–50	72	89	80	528.0	28.6	1.1	.9	P	N	N	9
24	11	38–42	…	…	…	…	…	…	…	…	…	…	7
25	9	43	281	195	144	2,827.0	164.2	.5	.7	D	RG	RG	7
26	9	47–52	139	46	103	747.2	59.6	.7	2.2	P	N	N	8
27	18	46–55	36	35	53	257.5	50.6	1.5	1.5	…	N	N	7
28	13	51	87	91	136	627.5	52.1	1.6	1.5	N	N	N	…
29	21	49–52	146	188	249	1,563.3	78.4	1.7	1.3	P	N	N	7
30	20	45–47	42	40	26	502.7	95.0	.6	.7	…	N	N	…
31	15	50	…	…	…	…	…	…	…	…	…	…	9
32	20	51–52	46	69	69	578.5	89.6	1.5	1.0	N	N	N	9
33	18	48–51	84	84	129	739.0	85.5	1.5	1.5	…	N	N	9
34	9		…	…	…	…	…	…	…	…	…	…	3
35	19	50	51	63	81	711.0	65.7	1.6	1.3	N	N	N	7
36	13	48–52	26	52	82	647.5	119.1	3.2	1.6	N	N	N	8
37	14	43–45	81	70	132	629.2	46.0	1.6	1.9	N	N	N	9
38	14	51	39	33	67	384.1	75.7	1.7	2.0	N	N	N	6
39	13	47	64	60	89	405.8	88.3	1.4	1.5	N	N	N	9
40	13	48–50	82	79	84	711.0	69.7	1.0	1.1	N	N	N	7
41	10	47–52	164	125	167	1,708.0	66.9	1.0	1.3	P	N	N	7
42	12	3–60	111	81	170	7,795.1	69.1	1.5	2.1	P	N	N	8
43	16	36	…	…	…	…	…	…	…	…	…	…	8
44	16	43	122	73	154	1,432.8	53.5	1.3	2.1	…	N	N	7
45	10	45	79	85	107	830.3	84.8	1.4	1.3	N	N	N	1
46	8	46–55	…	…	…	…	…	…	…	…	…	…	3
47	24	50–52	83	81	79	683.4	37.7	1.0	1.0	P	N	N	9
48	10	45–52	163	247	130	3,315.9	158.7	.8	.5	D	N	D	1
49	16	45–52	43	42	61	650.3	80.9	1.4	1.5	N	N	N	9
50	9	45–52	127	98	142	957.2	94.1	1.1	1.4	N	N	N	6

NOTE.—N = normal; D = deutan defect; P = protan defect; RG = red-green defect.

eight vectors spaced 45° apart to determine the discrimination ellipse around the same background chromaticity that had been used for the Trivector test. The staircases corresponding to these vectors were run in interleaved pairs, randomly chosen by the software. After the detection of the threshold in each vector, the ellipse was traced by interpolation, with use of the minimum squares method.

Inside the boundaries of the MacAdam ellipses, color discrimination is lost. This means that, the smaller the ellipse, the better the patient's discrimination ability. The quantitative parameters that are used to describe this ability are the ellipse length, the axis ratio, and the ellipse angle in color space. Ellipse length and angle are indicative of magnitude and type of color defect. We used ellipse area to quantify these changes, as an indicator of the patient's performance in color discrimination.

To confirm the type of red-green defect, the patients were also tested with the type I Neitz Anomaloscope (model OT-II [Neitz Instruments]), a standard test for the detection of red-green color defects.[40] The Neitz Anomaloscope determines the Rayleigh equation for the patient: the mixture of red (670 nm) and green (545

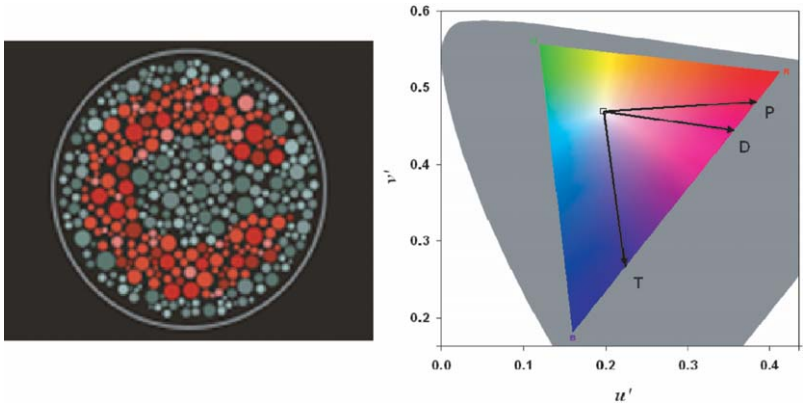

Figure 1. *Left,* Image of the stimulus provided by the CCT, showing the spatial and luminance noise (small patches of different diameters and luminances) and the letter "C" formed by the same patches at a chromaticity that differs from the background. *Right,* CIE chromaticity diagram (1976 $u'v'$) used by the CCT. The gray area indicates all colors seen by the human visual system, and the color triangle exhibits the chromaticities that can be displayed by the video monitor at the luminance level used in the tests. The lines P, D, and T correspond to the protan, deutan, and tritan, respectively, confusion lines tested in the Trivector protocol.

nm) light that matches a reference yellow (589 nm) light.[41] All three lights are produced by filters of equal luminance. The experimental procedure consisted of the observation of a circular horizontally bipartite field with 2° of visual angle. The yellow stimulus is in the lower hemifield, which can vary in luminance from dark to bright yellow. The task of the patient is to adjust the color of the upper hemifield to match the color and luminance of that presented at the lower hemifield. This is done by adjusting the proportion of the mixture of the green (545 nm) and red (670 nm) lights, whose combination is projected in the upper field. When both fields are matched in chromaticity, the luminance of the field is about 5 $cd \times m^{-2}$. The proportion used by trichromatic subjects with normal color vision is known from normative studies and was determined here for the control group. The exam was performed in a dark room, in accordance with the procedure recommended by the 1981 National Research Council Committee on Vision.[40]

The two pseudoisochromatic color plate tests, used in the genetic studies reported elsewhere,[26,27] were also used for the evaluation of color vision defects: Ishihara Test for Color Blindness (24 plates edition [Kanehara & Co.]) and AO H-R-R Pseudoisochromatic Plates (AO H-R-R [Richmond Products]). These tests consist of a series of printed plates with spatial and luminance noise forming a multicolored figure, which is also observed against a multicolored background. The only systematic difference between the figure and the background is the color. Patients with normal vision can detect the color differences between figure and the background, whereas patients with color defects fail to do it. The AO H-R-R test was built for the detection, classification, and quantification of red-green and blue-yellow defects. This test is made up of 24 boards in which colored circles of several sizes and luminances form figures in a background of gray circles also of several sizes and luminances. These figures are a cross, a circle, and a triangle. In the Ishihara test, there are numbers instead of figures. The patients were asked to read the numbers in 6 s. This response time was a slight adaptation made after consideration of the characteristics of the study group. The Ishihara test detects only protan and deutan defects and enables a more precise differentiation between both kinds of defects.

Response Reliability

The CCT software incorporates a reliability-testing procedure with catch trials, which present a saturated color at the maximum of the cathode ray tube gamut. These catch trials are presented at different times in the test session and constitute ~10% of the stimuli. For the Trivector, one color was used in the catch trial (CIE 1976 coordinates: $u' = .119$; $v' = .391$; vector length 1,100 $u'v'$ units); for the ellipses, another chromaticity was used (CIE 1976 coordinates: $u' = .308$; $v' = .469$; vector length 1,100 $u'v'$ units). These saturated colors are discriminated even by patients with severe color vision impairment. This procedure tests the ability of the subject to respond correctly to the target, which depends on the understanding of instructions and on the attention directed to the task during the testing session. We define the percentage of correct responses to these catch trials as a measure of reliability. Reliability was 100% for both control subjects and patients with DMD—that is, there were no mistakes in the catch trials. This means that the subjects were performing the required task correctly during the entire length of the testing session.

Statistical Analysis

Statistical analysis was performed with the software Statistica (StatSoft v.6). Statistical differences among the groups were verified with the χ^2 test, the Mann-Whitney U test, and the Kruskal-Wallis analysis of variance (ANOVA) by ranks. We use the Tukey honest significance difference (HSD) design for unequal N, to determine the significant differences between group means in the ANOVA setting. The Wilcoxon test was used to assess differences in the Ishihara and AO H-R-R categorical color vision classification. The Spearman rank test correlation was used to verify the relationship between color vision results and the other variables—age and Vignos score. A cluster analysis was performed by measuring a Euclidian distance in a complete linkage rule, to verify similarities and dissimilarities among parameters of the color vision tests, Vignos score, and gene deletion. Adhesion to the normal distribution was checked with the Kolmogorov-Smirnov test.

Results

The battery of color tests could be performed in 88% (44/50) of the patients with DMD. The remaining six patients with DMD had difficulty understanding or performing the task in the CCT and were excluded from our analysis. The Anomaloscope test was performed in 77% (34/44) of the remaining patients with DMD. The color vision results are shown in tables 1 and 2 (rightmost columns). One patient with DMD (table 1, number 6) had a congenital dichromatic defect classified as deuteranopia and was excluded from our statistical analysis.

Color discrimination results from subjects with DMD and controls in the CCT Trivector (fig. 2) showed significant differences in the Kruskal-Wallis ANOVA for all three color confusion axes (protan $H = 27.216$, $P < .001$; deutan $H = 30.232$, $P < .001$; tritan $H = 19.005$, $P < .001$). In addition, MacAdam ellipses areas obtained with the CCT had larger areas in the patients with DMD compared with the controls ($H = 27.302$, $P < .001$).

For the CCT Trivector axes, we calculated the tritan/protan (T/P) and tritan/deutan (T/D) ratios. For the controls, the tritan thresholds are always higher compared with the thresholds of the protan and deutan thresholds, because of distortions of the CIE color space. Alterations in these ratios compared with those of the controls might be used as an indication of color vision anomaly, even if each of the color discrimination thresholds are within the normal tolerance limits. Furthermore, alterations in these ratios are indicative of the type of anomaly. No alteration occurs if the anomaly is diffuse—that is, if there is a uniform change in thresholds. Other patterns reveal specific losses.

For controls, the mean value of the T/P ratio was 1.68 (SD 0.36), and that of the T/D ratio was 1.69 (SD 0.40). For the patients with DMD, the T/P and T/D ratios of the patients with normal thresholds in all Trivector axes, with consideration of the tolerance limits calculated for the control group, were considered. The mean T/P ratio was 1.40 (SD 0.40), and the mean T/D ratio was 1.43 (SD 0.44) for patients with DMD. A statistically significant difference was found between controls and patients with DMD for the T/P (Mann-Whitney U test: $U = 998.90$, $P < .003$) and for T/D ($U = 1{,}003.90$, $P = .005$) ratios. This reduction of the T/P and T/D ratios indicates a red-green defect, since it results from the fact that the mean thresholds for the protan and deutan axes were elevated relative to the mean tritan threshold.

Table 2. Age versus Color Thresholds Product-Moment Correlation Index

Study Group	Protan		Deutan		Tritan	
	r	*P*	*r*	*P*	*r*	*P*
Controls	−.568	<.001	−.463	<.001	−.479	<.001
DMD	−.390	.004	−.266	NS	−.243	NS
Up 30[a]	−.758	.006	−.281	.004	−.606	.047
Down 30[b]	−.551	.002	−.408	.020	−.395	.025

NOTE.—NS = no statistical significance.
[a] Gene deletion upstream of exon 30.
[b] Gene deletion downstream of exon 30.

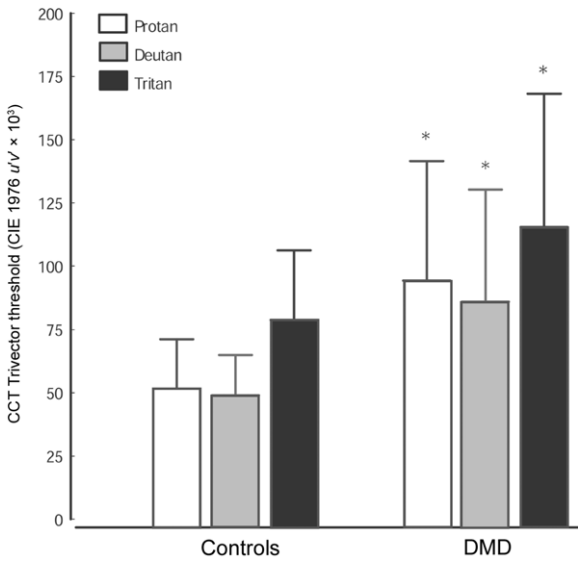

Figure 2. Color discrimination thresholds of the patients with DMD and control subjects (mean ± SD) for the protan, deutan, and tritan confusion lines of the Trivector test. Statistical difference was significant for all three confusion lines.

A red-green color defect was found in 47% (21/44) of the patients with DMD in the CCT. These results were confirmed by the Rayleigh equation, obtained with the Neitz Anomaloscope. A χ^2 test showed that there was no difference between the classifications of the color vision defect based on the CCT and on the Anomaloscope ($\chi^2 = 0.680$, $P = .495$). Diffuse defects were found in 3/44 (7%) patients.

The Ishihara and AO H-R-R color vision tests detected color vision alterations in fewer patients: the AO H-R-R was able to identify only 3 of 44 (7%), and the Ishihara 2 of 44 (5%), of red-green color vision losses in patients with DMD. In all these cases, a red-green color defect was also detected by the CCT.

A categorical comparison (Wilcoxon test) of color defects obtained with the Ishihara and with the CCT shows that the two tests differ in the ability to detect color defects ($W = -26.000$, $P = .026$). The same comparison between the AO H-R-R test and the CCT also shows that the results of the two tests differ even more significantly ($W = -95.000$, $P < .001$). The same analysis was made to compare the Ishihara and the AO H-R-R color vision classification with the Neitz Anomaloscope. It showed that these two tests have a lower sensitivity to detect red-green color defects than the Anomaloscope (Ishihara, $W = -20.000$, $P = .021$; AO H-R-R, $W = -94.000$, $P = .009$).

Color vision thresholds of the control subjects decreased with increasing age, from 9 to 21 years, confirming an improvement in discrimination capacity during this age

period, as shown in the literature.[42] This improvement was also observed in the patients with DMD. Spearman rank order correlations between color thresholds and age were negative and statistically significant for the three CCT Trivector thresholds and for the ellipses area (table 2).

To describe quantitatively the relationship between the color vision result parameters and the genotype variables—region of the gene deletion—we performed a cluster analysis, measuring Euclidian distance in a complete linkage rule. Two clusters were found: one cluster was formed by the area results of the CCT ellipses, and another cluster linked the CCT results with the region of the genetic deletion. In the latter, there are two segregations. The first shows proximity among the region of the gene deleted with the T/P and T/D ratio. The second cluster connects the CCT Trivector results and CCT ellipses angle. Both clusters had an insignificant distance as compared with the CCT ellipses area result.

Since the cluster analysis reveals that there is an association between the CCT color vision results and the region of gene deletion, we analyzed statistical significances considering this parameter. The criterion to separate the DMD patients in groups was based on the ERG studies that showed that exon 30 is essential for normal retina electrophysiology.[14,25,43]

Figure 3 shows color vision deficiencies found in the patients with DMD with known deletions, including the patient with congenital color defect excluded previously. In panel A, we see that all patients except one have deletions downstream of exon 30. Of 19 patients with normal color vision, 8 have deletions downstream of exon 30, and 11 have deletions upstream of exon 30. These data are summarized in figure 3*B*.

Patients with DMD were therefore stratified into two subgroups according to gene deletion: those with deletion downstream of exon 30 ($n = 32$) and those with deletion upstream of exon 30 ($n = 11$). There was a high percentage (66% [21/32]) of red-green defects in the patients with deletions downstream of exon 30, whereas color defects were not found in any of the patients with deletions upstream of exon 30, except for a patient with deuteranopia who was previously excluded.

Statistical difference in the Kruskal-Wallis ANOVA test was found for the CCT Trivector protan ($H = 25.418$, $P < .001$), deutan ($H = 31.342$, $P < .001$), and tritan ($H = 17.468$, $P < .001$) thresholds (fig. 4) and for the CCT ellipses area ($H = 31.765$, $P < .001$) (fig. 5). These differences were between controls and patients with DMD with deletions downstream of exon 30 (Tukey post hoc analysis). No statistical difference was found between the controls and the patients with DMD with deletions upstream of exon 30.

A statistically significant difference was also found between controls and patients with DMD with deletions downstream of exon 30 for the T/P ratio ($H = 11.978$, $P = .003$) and for the T/D ratio ($F = 11.281$, $P = .004$). All T/P and T/D ratios are shown in table 3.

The improvement of color discrimination with age was confirmed for both subgroups of patients with DMD with gene deletion upstream and downstream of exon 30. The Spearman rank-order correlation data showed reduction in CCT Trivector thresholds and ellipses area as ages increased (see table 2).

Discussion

Here we report, for the first time to our knowledge, that red-green color vision defect is highly prevalent in patients with DMD with deletions downstream of exon 30. Since all but one (11/12) of the patients with deletions upstream of exon 30 had normal color vision, the present study suggests that the color defect is related to possible functional damage associated with Dp260, the dystrophin isoform located in the outer plexiform layer.[6,14–20,22] Previous studies on evaluation of visual functions in patients with DMD reported normal ophthalmologic conditions as well as visual functions, including visual acuity, ocular motility, and color vision.[19,27,44] However, various degrees of retinal impairment had been found in electrophysiological evaluations. The full-field ERG of patients with DMD showed alterations in scotopic and photopic responses.[6,15,16,18,19,22–25,43,45–50] Indications of impairment in the visual pathways were also observed using visual evoked potential (VEP) techniques. Benoff et al.[47] investigated the contrast sensitivity mediated by magno- and parvocellular pathways isolating the responses of the "ON" and "OFF" subsystems of the visual pathway. They found impairment in the contrast sensitivity mediated by the magnocellular-ON pathway in patients with DMD. In a multimodal evoked potential assessment, Girlanda et al.[50] found reductions for the VEP of patients with DMD and BMD, but not for other modalities, including somatosensory and auditory evoked potentials.

The lack of agreement between the functional evaluations of vision and the electrophysiological studies reported above might be due to the use of procedures that were not sufficiently sensitive to detect functional impairment. We therefore decided to assess visual function with sensitive instruments and focused the present study on color vision.

With the instruments used, we were able to demonstrate that color vision impairment in patients with DMD is highly prevalent. Not only was the incidence of color vision defect very high, but it was also selective and was confirmed by two independent and very different tests. The CCT—a quantitative and sensitive test—showed that patients with DMD had a red-green defect, and this result was confirmed by the gold standard used to measure red-green color defect, the Neitz Anomaloscope. The incidence of color vision defect among the patients with DMD was 54% (24/44); of these 24 patients, 21 had losses of the red-green type, whereas only 3, or 7%, had diffuse color vision loss. This is a much higher proportion than

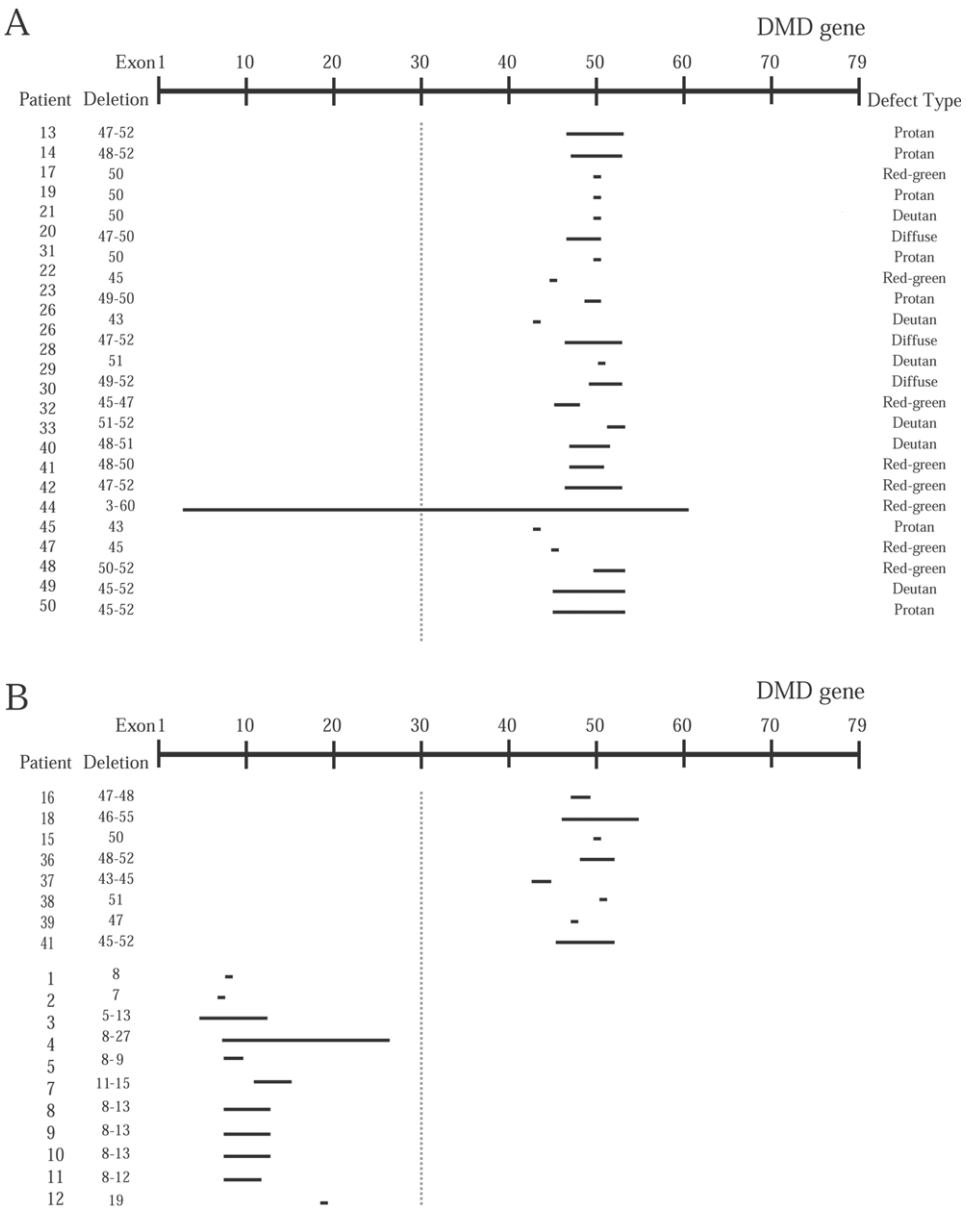

Figure 3. Patients with DMD stratified according to their color vision deficiencies, with their region of dystrophin gene deletion shown. The range of deletion is indicated numerically in the first column. For each patient, the length of the DMD gene is shown by a horizontal black line that represents the extension and location of deletion in this gene. *A,* All the patients with color vision impairment. All patients had deletions downstream of exon 30. *B,* Patients with normal color vision classification. The majority have deletions upstream of exon 30.

expected for congenital protan and deutan defects, which occur in ~7%–10% of the male population.[40,51]

The mechanisms underlying this color vision loss are not known. Patients with DMD present selective impairment in a function mediated by a specific neural pathway—the parvocellular pathway, which mediates red-green color vision. This pathway is initiated by the response of the L and M cones and comprises a neural network from the retina to the lateral geniculate nucleus and, from there, to several cortical levels. The magnocellular pathway, which mediates achromatic functions, is also initiated by inputs from the L and M cones.[52] In the magnocellular pathway, the signals from the L and M cones are added to convey the information of luminance, whereas, in the parvocellular pathway, the M and L signals are compared, and the neural response expresses their difference, to convey the chromatic information. Chromatic processing includes, in addition, the blue-yellow pathway in which the S-cone signals are compared with the added inputs of the L and M cones.[53]

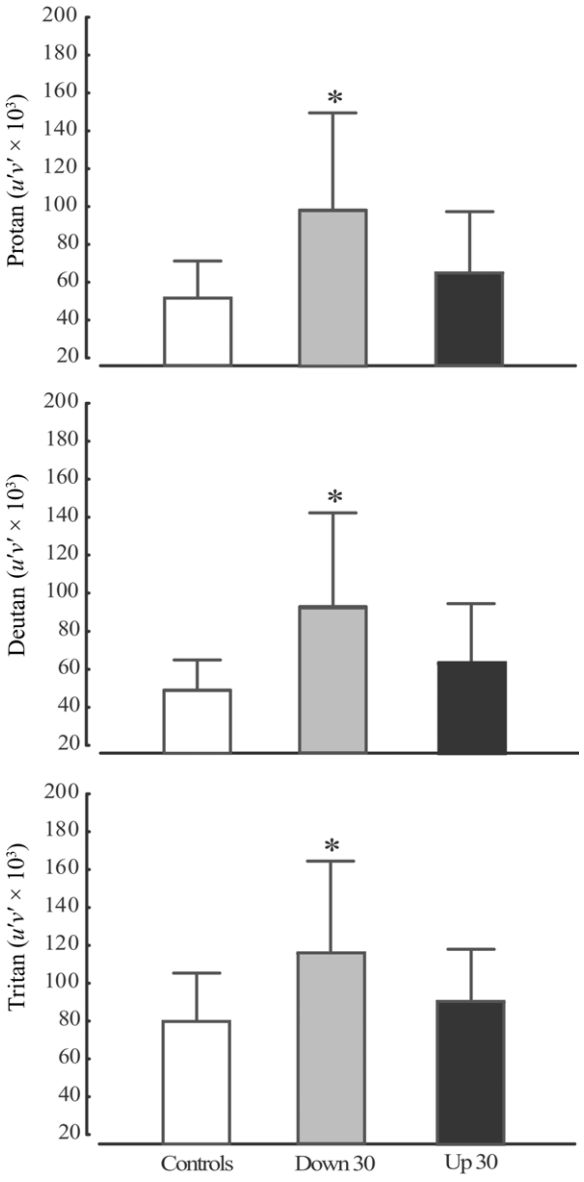

Figure 4. Color discrimination results for the control subjects and patients with DMD, grouped according the region of the gene deletion (mean ± SD) for protan, deutan, and tritan confusion lines. Statistical difference was found between the controls and the patients with deletion downstream of exon 30, for all the confusion lines.

Our findings differ from the result of the work of Benoff et al.,[47] who showed that there was magnocellular but not parvocellular impairment in the VEPs of patients with DMD. This disagreement could be due to two factors: (1) The magnocellular pathway is tuned to detect luminance stimuli as the checkboard stimuli that varied in the size of the elements and in the contrast level used in that study. Although the parvocellular pathway also exhibits a response to luminance stimuli, the chromatic stimuli, either red or green, produces the most vigorous activation. (2) The magnocellular pathway collects the response of many more cones than the parvocellular pathway. Since the VEP is a cortical mass response of small amplitude, differences could be more evident in responses mediated by the magnocellular rather than parvocellular pathway.

In the patients with DMD, we found losses mainly in the red-green pathway. These losses may originate in the photoreceptors, since it has been demonstrated by Ueda et al.[12,13] that dystrophin is located within the invagination of the presynaptic photoreceptor terminal. These invaginated synapses are composed of two lateral processes from horizontal cells and one central process from the ON-bipolar cell, which constitutes a synaptic triad contributing to build the ON visual pathway. If the color defect originates in the photoreceptors, there should be a reduction in all three pathways. In addition to the parvocellular pathway, which mediates red-green color vision, both the magnocellular and koniocellular functions should be affected, since L and M cones constitute inputs in these pathways as well as in the parvocellular pathway. The VEP magnocellular-ON impairment[47] and the ERG ON-pathway impairment[6,15] found in patients with DMD provide functional evidence in favor of this hypothesis.

The vertebrate visual system has a functional separation of neural pathways that signal ON and OFF responses to light. The ON cells signal in response to illumination, and the OFF cells signal when light is turned off. These pathways are organized in a concentric center-surround antagonism: an excitatory center and an inhibitory surround

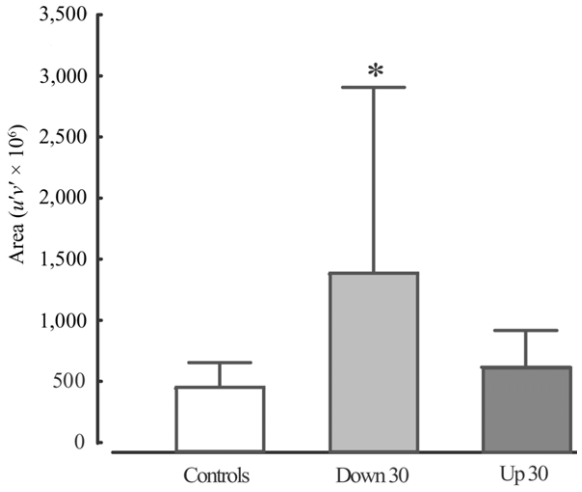

Figure 5. The mean area of the CCT ellipses for controls and for the patients with DMD stratified into two groups: those with deletion downstream or upstream of exon 30. The area of color discrimination ellipses quantify the ability of the subject to discriminate color in all directions around a point in the chromaticity diagram. The smaller the area, the better the discrimination. The downstream group shows statistically significant wider ellipses areas or reduction in color discrimination, compared with the other two groups.

Table 3. T/P and T/D Trivector Confusion-Axes Ratios

Study Group	T/P	T/D
Controls	1.69 (.37)	1.70 (.41)
DMD		
Up 30[a]	1.58 (.20)	1.67 (.28)
Down 30[b]	1.25 (.31)	1.18 (.28)

NOTE.—Values are given as means (SDs).
[a] Gene deletion upstream of exon 30.
[b] Gene deletion downsteam of exon 30.

or vice-versa.[54] The main reason for the presence of ON and OFF channels in the visual system could be to optimize information about increments and decrements of light to the CNS. The same arrangement occurs in the processing of chromatic stimuli, in which ON and OFF signals are generated in response to opponent colors.

Accordingly, the red-green color pathway in the retina has its bipolar and ganglion cells arranged in two types of receptive fields with center-surround spatial antagonism of the L and M cones: L-ON versus M-OFF, and L-OFF versus M-ON.[53,55–57] Since the previous literature shows selective impairment of the ON pathway, it is possible that the color vision defect that we report could be reflecting the impairment of only the ON-pathway.

The understanding of the S-cone color processing in the retina is limited, and the existence of the S-OFF cone pathway in the retina is not established.[53,58] The study by Calkins[59] shows that the ON bipolar cells make contact with S cones in two different ways: there are the characteristic ON-type invaginating contacts and, in addition, other numerous semi-invaginating contacts with the S cones. Since dystrophin would affect the invaginating contacts because of its location near the synaptic ribbon, it might not influence the physiology of these ON bipolars, because most of their contacts with the S cone are located close to but not directly in the invaginating region. This could explain why the patients with DMD had normal tritan thresholds.

The present finding of an association between DMD and red-green color defect in ~47% of the affected patients constitutes a new finding in the area of DMD studies. The only study that evaluated color vision of the patients with DMD is that of Sigesmund et al.,[27] who conducted a complete ophthalmologic evaluation including biomicroscopy, cycloplegic refraction, fundoscopy, prism and cover test, ERG, and tests of color vision, stereoacuity, and visual acuity in 21 patients with a diagnosis of DMD and 5 patients with BMD. Color vision was evaluated in 17 of 21 patients with the use of AO H-R-R, the Ishihara Color Plates, or the Farnsworth D-15 tests. All patients tested had normal color vision, except for one with a severe red-green defect. This patient had a deletion downstream of exon 30. Since most patients had normal color vision, extraocular muscle function, stereoacuity, and visual acuity, the authors[27] concluded that patients with DMD have normal vision.

The discrepancy between our data showing a high prevalence of red-green color defect in patients with DMD and the study by Sigesmund et al.[27] is probably due to the low sensitivity of the traditional color tests used in that study. Indeed, our results of color vision defect in patients with DMD evaluated with the Ishihara and the AO H-R-R plate tests are in accordance with the results found by these authors[27] and with the expected proportion for congenital color defect in the population. The results obtained here benefitted from a new method for the measurement of color discrimination, developed in the early 1990s,[39] whose norms were provided by Ventura et al.[32] This new procedure has demonstrated a better capacity than the traditional tests to detect color vision defects in retinal pathologies like glaucoma and in hypertension,[35] Parkinson disease,[60] nonretinopathic diabetes,[31] and mercury intoxication,[34] as well as in genetic diseases like dominant optic atrophy[61] and Leber's hereditary optic neuropathy.[62]

The psychophysical (staircase) method employed and the four-alternative forced-choice task used by the CCT made possible a precise quantification of the color discrimination threshold. The use of the Neitz Anomaloscope, which is the gold standard to identify and classify red-green color defects, reinforced and confirmed the existence of the selective red-green color discrimination defect in the patients in this study.

The cluster analysis performed on our data revealed a strong association between the color thresholds obtained in the CCT Trivector and the region of gene deletion. Although the full-field ERG shows great variability in patients with DMD, a relationship of these electrophysiological losses with the gene-deletion region was not verified by some authors,[19,22] whereas other studies were able to show a genotype-phenotype correlation[6,14,15,20,25] in which the patients with DMD who had the gene deletion downstream of exon 30 had the more preeminent reduction in the ERG b-wave amplitude. The latter studies, therefore, strongly suggested that the dystrophin isoform Dp260 is required for normal retinal function. Our color vision results are in line with those electrophysiological results, since the cluster amalgamation shows that color thresholds have a high level of aggregation with the region of the gene deletion.

The apparent relationship between the region of gene deletion and color vision defects in patients with DMD can be seen in figure 5. This figure shows the region of gene deletion in each patient, stratifying them into two subgroups according to their red-green color vision results: those with impaired color vision (fig. 5*A*) and those with normal color vision (fig. 5*B*). Red-green color defect was present in 47% (21/44) of patients with deletion downstream of exon 30.

Anomaloscope results from some patients with DMD that indicated a discrete anomalous trichromacy were not in agreement with the CCT Trivector thresholds, which were within the normal limits in the CCT for those patients. However, their T/P and T/D ratios were lower (~1.0) than those of normal subjects (~1.7). These threshold ra-

tios might offer an index to be checked before considering patients' vision as normal or color defective.

An interesting question is how do these color vision losses impact the daily life of the patient? We would call these subclinical symptoms, since they are not materialized into complaints. Subjects learn to live with less-than-perfect, or defective, color vision. Even individuals with extreme dichromatism often do not find out about their disadvantage until they are adults. A person who has never been faced with another reality has difficulties realizing that she or he is missing information from the world, unless confronted with specific tasks that reveal the loss. This is the basis and motivation of color vision testing—to create situations in which the chromatic discrimination can be isolated. Interestingly, our previous experience in color vision testing in several other pathologies[31–34,63–65] showed that very few patients verbalize or are aware of their difficulty to discriminate color or that they have a deficiency.

The improvement of color discrimination with age observed in controls reflects the normal development of this function that reaches its maximum around age 18 years.[42] The patients with DMD also showed improvement in color discrimination measured by the CCT. This finding could be interpreted as evidence that the color defect is nonprogressive in patients with DMD.

Possible cognitive and motor function influences in the assessment of visual function were minimized in our results, since the CCT and Neitz Anomaloscope tasks are cognitively simple and, in the CCT, button-pressing responses were not required for patients with severe motor impairment. We excluded the six patients who had difficulty understanding the CCT instructions. Response reliability was measured in the remaining 44 patients by the assessment of correct responses to a control stimulus that showed a saturated color. There were no errors, showing that these patients were paying attention to the stimulus and were capable of making the discrimination required in the test.

In conclusion, with the battery of tests that we used, not only was it possible to identify the existence of losses in color discrimination, but we were also able to show that these losses were selective for the red-green axis, an observation still not understood.

Acknowledgments

We thank ABDIM for providing space, referring patients and respective genetic information, and performing the evaluation of motor function for this study. We are also very grateful to Dr. Maria Rita Passos-Bueno, Dr. Mariz Vainzof, Dr. Rita C. M. Pavanello, and Antonia Cerqueira, from the Human Genome Research Center, for the clinical and molecular study of the patients with DMD. This research was supported by Fundação de Amparo à Pesquisa do Estado de São Paulo (FAPESP) Projeto Temático grant 02/12733-8, Conselho Nacional de Desenvolvimento Científico e Tecnológico (CNPq) grant 523303/95-5 (to D.F.V.), and Centro de Pesquisa, Inovação e Divulgação–FAPESP (Centro de Estudos do Genoma Humano) (to M.Z.). D.F.V. and M.Z. are CNPq research fellows.

Web Resource

The URL for data presented herein is as follows:

Online Mendelian Inheritance in Man (OMIM), http://www.ncbi.nlm.nih.gov/Omim/ (for DMD)

References

1. Matsuo M (1996) Duchenne/Becker muscular dystrophy: from molecular diagnosis to gene therapy. Brain Dev 18:167–172
2. Nobile C, Marchi J, Nigro V, Roberts RG, Danieli GA (1997) Exon-intron organization of the human dystrophin gene. Genomics 45:421–424
3. O'Brien KF, Kunkel LM (2001) Dystrophin and muscular dystrophy: past, present, and future. Mol Genet Metab 74:75–88
4. Hoffman EP, Brown RH Jr, Kunkel LM (1987) Dystrophin: the protein product of the Duchenne muscular dystrophy locus. Cell 51:919–928
5. Koenig M, Monaco AP, Kunkel LM (1988) The complete sequence of dystrophin predicts a rod-shaped cytoskeletal protein. Cell 53:219–226
6. Pillers DA, Fitzgerald KM, Duncan NM, Rash SM, White RA, Dwinnell SJ, Powell BR, Schnur RE, Ray PN, Cibis GW, et al (1999) Duchenne/Becker muscular dystrophy: correlation of phenotype by electroretinography with sites of dystrophin mutations. Hum Genet 105:2–9
7. Schmitz F, Drenckhahn D (1997) Localization of dystrophin and beta-dystroglycan in bovine retinal photoreceptor processes extending into the postsynaptic dendritic complex. Histochem Cell Biol 108:249–255
8. Claudepierre T, Dalloz C, Mornet D, Matsumura K, Sahel J, Rendon A (2000) Characterization of the intermolecular associations of the dystrophin-associated glycoprotein complex in retinal Muller glial cells. J Cell Sci 113:3409–3417
9. Claudepierre T, Mornet D, Pannicke T, Forster V, Dalloz C, Bolanos F, Sahel J, Reichenbach A, Rendon A (2000) Expression of Dp71 in muller glial cells: a comparison with utrophin- and dystrophin-associated proteins. Invest Ophthalmol Vis Sci 41:294–304
10. Connors NC, Kofuji P (2002) Dystrophin Dp71 is critical for the clustered localization of potassium channels in retinal glial cells. J Neurosci 22:4321–4327
11. Schmitz F, Drenckhahn D (1997) Dystrophin in the retina. Prog Neurobiol 53:547–560
12. Ueda H, Baba T, Terada N, Kato Y, Tsukahara S, Ohno S (1997) Dystrophin in rod spherules; submembranous dense regions facing bipolar cell processes. Histochem Cell Biol 108:243–248
13. Ueda H, Tsukahara S, Kobayashi T, Ohno S (1995) Immunocytochemical study of dystrophin-related protein in the rat retina. Ophthalmic Res 27:219–226
14. Pillers DA, Bulman DE, Weleber RG, Sigesmund DA, Musarella MA, Powell BR, Murphey WH, Westall C, Panton C, Becker LE, et al (1993) Dystrophin expression in the human retina is required for normal function as defined by electroretinography. Nat Genet 4:82–86
15. Pillers DM, Sigesmund DA, Ray PN, Musarella MA, Tremblay

F, Seltzer WK, Powell B, Mccabe ERB, Schnur RE, Panton C, et al (1993) Genotype-phenotype correlations identified by electrophysiology of the retina in Duchenne and Becker muscular-dystrophy patients. Am J Hum Genet Suppl 53:A146
16. Fitzgerald KM, Cibis GW, Harris DJ, Rothberg PG (1993) On-responses and off-responses of the photopic ERG in Duchenne muscular-dystrophy and congenital stationary night blindness. Invest Ophthalmol Vis Sci 34:1076
17. Fitzgerald KM, Cibis GW, Gettel AH, Rinaldi R, Harris DJ, White RA (1999) ERG phenotype of a dystrophin mutation in heterozygous female carriers of Duchenne muscular dystrophy. J Med Genet 36:316–322
18. Tremblay F, De Becker I, Riddell DC, Dooley JM (1994) Duchenne muscular dystrophy: negative scotopic bright-flash electroretinogram and normal dark adaptation. Can J Ophthalmol 29:280–283
19. De Becker I, Riddell DC, Dooley JM, Tremblay F (1994) Correlation between electroretinogram findings and molecular analysis in the Duchenne muscular-dystrophy phenotype. Br J Ophthalmol 78:719–722
20. D'Souza VN, Nguyen TM, Morris GE, Karges W, Pillers DA, Ray PN (1995) A novel dystrophin isoform is required for normal retinal electrophysiology. Hum Mol Genet 4:837–842
21. Drenckhahn D, Holbach M, Ness W, Schmitz F, Anderson LV (1996) Dystrophin and the dystrophin-associated glycoprotein, beta-dystroglycan, co-localize in photoreceptor synaptic complexes of the human retina. Neuroscience 73:605–612
22. Pascual Pascual SI, Molano J, Pascual-Castroviejo I (1998) Electroretinogram in Duchenne/Becker muscular dystrophy. Pediatr Neurol 18:315–320
23. Yang Y, Zhang C, Sheng W, Pan S, Wu D, Jiang F (2001) Correlation between electroretinographic findings, clinical phenotypic and genotypic analysis in Duchenne and Becker muscular dystrophy. Zhonghua Yi Xue Yi Chuan Xue Za Zhi 18:32–34
24. Green DG, Guo H, Pillers DA (2004) Normal photoresponses and altered b-wave responses to APB in the mdxCv3 mouse isolated retina ERG supports role for dystrophin in synaptic transmission. Vis Neurosci 21:739–747
25. Pillers DAM, Weleber RG, Green DG, Rash SM, Dally GY, Howard PL, Powers MR, Hood DC, Chapman VM, Ray PN, et al (1999) Effects of dystrophin isoforms on signal transduction through neural retina: genotype-phenotype analysis of Duchenne muscular dystrophy mouse mutants. Mol Genet Metab 66:100–110
26. Zatz M, Itskan SB, Sanger R, Frota-Pessoa O, Saldanha PH (1974) New linkage data for the X-linked types of muscular dystrophy and G6PD variants, colour blindness, and Xg blood groups. J Med Genet 11:321–327
27. Sigesmund DA, Weleber RG, Pillers DA, Westall CA, Panton CM, Powell BR, Heon E, Murphey WH, Musarella MA, Ray PN (1994) Characterization of the ocular phenotype of Duchenne and Becker muscular dystrophy. Ophthalmology 101: 856–865
28. Birch EE, O'Connor AR (2001) Preterm birth and visual development. Semin Neonatol 6:487–497
29. Birch J (2001) Diagnosis of defective colour vision. Buttenworth-Heinemann, Oxford, United Kingdom
30. Mollon JD, Reffin JP (1989) A computer-controlled colour vision test that combines the principles of Chibret and of Stilling. J Physiol Lond 414:5
31. Ventura DF, Costa MF, Gualtieri M, Nishi M, Bernick M, Bonci DM, de Souza J (2003) Early vision loss in diabetic patients assessed by the Cambridge Colour Test. In: Mollon JD, Pokorny J, Knoblauch K (eds) Normal and defective colour vision, 1st ed. Oxford University Press, New York, pp 395–403
32. Ventura DF, Silveira LC, Rodrigues AR, de Souza J, Gualtieri M, Bonci DM, Costa MF (2003) Preliminary norms for the Cambridge Colour Test. In: Mollon JD, Pokorny J, Knoblauch K (eds) Colour and defective colour vision, 1st ed. Oxford University Press, New York, pp 331–339
33. Ventura DF, Costa MTV, Costa MF, Berezovsky A, Salomao SR, Simoes AL, Lago M, Pereira LHMC, Faria MAM, de Souza JM, et al (2004) Multifocal and full-field electroretinogram changes associated with color-vision loss in mercury vapor exposure. Vis Neurosci 21:421–429
34. Ventura DF, Simoes AL, Tomaz S, Costa MF, Lago M, Costa MTV, Canto-Pereira LHM, de Souza JM, Faria MAM, Silveira LCL (2005) Colour vision and contrast sensitivity losses of mercury intoxicated industry workers in Brazil. Environ Toxicol Pharmacol 19:523–529
35. Castelo-Branco M, Faria P, Forjaz V, Kozak LR, Azevedo H (2004) Simultaneous comparison of relative damage to chromatic pathways in ocular hypertension and glaucoma: correlation with clinical measures. Invest Ophthalmol Vis Sci 45:499–505
36. Chamberlain JS, Gibbs RA, Ranier JE, Nguyen PN, Caskey CT (1988) Deletion screening of the Duchenne muscular dystrophy locus via multiplex DNA amplification. Nucleic Acids Res 16:11141–11156
37. Beggs AH, Koenig M, Boyce FM, Kunkel LM (1990) Detection of 98% of DMD/BMD gene deletions by polymerase chain reaction. Hum Genet 86:45–48
38. Vignos PJ Jr (1967) Diagnosis of progressive muscular dystrophy. J Bone Joint Surg Am 49:1212–1220
39. Regan BC, Reffin JP, Mollon JD (1994) Luminance noise and the rapid determination of discrimination ellipses in colour deficiency. Vision Res 34:1279–1299
40. Pokorny J (1981) Procedures for testing colour vision—report of working group 41. Committee on Vision, Assembly of Behavioral and Social Sciences, National Research Council. National Academy Press, Washington D.C.
41. Siegel IM (1981) The X-Chrom lens: on seeing red. Surv Ophthalmol 25:312–324
42. Knoblauch K, Vital-Durand F, Barbur JL (2001) Variation of chromatic sensitivity across the life span. Vision Res 41:23–36
43. Fitzgerald KM, Cibis GW, Giambrone SA, Harris DJ (1994) Retinal signal transmission in Duchenne muscular dystrophy: evidence for dysfunction in the photoreceptor depolarizing bipolar cell pathway. J Clin Invest 93:2425–2430
44. Sigesmund DA, Ray PN, Pillers DM, Weleber RG, Westall CA, Panton CM, Musarella MA (1993) Duchenne muscular-dystrophy (dmd): severity of rod dysfunction correlates with location of deletion in dmd gene. Invest Ophthalmol Vis Sci 34:1463
45. Pillers DA, Weleber RG, Woodward WR, Green DG, Chapman VM, Ray PN (1995) mdxCv3 mouse is a model for electroretinography of Duchenne/Becker muscular dystrophy. Invest Ophthalmol Vis Sci 36:462–466
46. Cibis GW, Fitzgerald KM, Harris DJ Rothberg PG, Rupani M (1993) The effects of dystrophin gene mutations on the ERG in mice and humans. Invest Ophthalmol Vis Sci 34:3646–3652

47. Benoff K, Fitzgerald K, Zemon V, Pinkhasov E, Gordon J, Cibis G (2001) Magnocellular ON-pathway deficits in Duchenne muscular dystrophy: a visual evoked potential study. Invest Ophthalmol Vis Sci 42:S787
48. Fitzsimmons JS, McLachlan JI, Reeves WG, Marriott DW, Woolfson AM, Mayhew J (1980) Carrier detection in Duchenne muscular dystrophy. J Med Genet 17:165–169
49. Ino-ue M, Honda S, Nishio H, Matsuo M, Nakamura H, Yamamoto M (1997) Genotype and electroretinal heterogeneity in Duchenne muscular dystrophy. Exp Eye Res 65:861–864
50. Girlanda P, Quartarone A, Buceti R, Sinicropi S, Macaione V, Saad FA, Messina L, Danieli GA, Ferreri G, Vita G (1997) Extramuscle involvement in dystrophinopathies: an electroretinography and evoked potential study. J Neurol Sci 146:127–132
51. Neitz M, Neitz J (2000) Molecular genetics of color vision and color vision defects. Arch Ophthalmol 118:691–700
52. Dobkins KR, Gunther KL, Peterzell DH (2000) What covariance mechanisms underlie green/red equiluminance, luminance contrast sensitivity and chromatic (green/red) contrast sensitivity? Vision Res 40:613–628
53. Lee BB (2004) Paths to colour in the retina. Clin Exp Optom 87:239–248
54. Schiller PH (1995) The ON and OFF channels of the mammalian visual system. Prog Retin Eye Res 15:173–195
55. De Valois RL, Abramov I, Jacobs GH (1966) Analysis of response patterns of LGN cells. J Opt Soc Am 56:966–977
56. Diller L, Packer OS, Verweij J, McMahon MJ, Williams DR, Dacey DM (2004) L and M cone contributions to the midget and parasol ganglion cell receptive fields of macaque monkey retina. J Neurosci 24:1079–1088
57. De Valois RL, Cottaris NP, Elfar SD, Mahon LE, Wilson JA (2000) Some transformations of color information from lateral geniculate nucleus to striate cortex. Proc Natl Acad Sci USA 97:4997–5002
58. Dacey DM, Packer OS (2003) Colour coding in the primate retina: diverse cell types and cone-specific circuitry. Curr Opin Neurobiol 13:421–427
59. Calkins DJ (2001) Seeing with S cones. Prog Retin Eye Res 20: 255–287
60. Regan BC, Freudenthaler N, Kolle R, Mollon JD, Paulus W (1998) Colour discrimination thresholds in Parkinson's disease: results obtained with a rapid computer-controlled colour vision test. Vision Res 38:3427–3431
61. Simunovic MP, Votruba M, Regan BC, Mollon JD (1998) Colour discrimination ellipses in patients with dominant optic atrophy. Vision Res 38:3413–3419
62. Ventura DF, Silveira LCL, Nishi M, Costa MF, Gualtieri M, Santos RMA, Pinto CT, Moura ALA, Rodrigues AR, Sakurada C, et al (2004) Color vision loss in patients treated with chloroquine. Arq Bras Oftalmol 66:9–15
63. Costa MF, Ventura DF, Perazzolo F, Murakoshi MT, Silveira LCL (2006) Absence of binocular summation, eye dominance and learning effects in color discrimination. Vis Neurosci 23: 461–469
64. Ventura DF, Quiros P, Carelli V, Salomao SR, Gualtieri M, Oliveira AG, Costa MF, Berezovsky A, Sadun F, De Negri AM, et al (2005) Chromatic and luminance contrast sensitivities in asymptomatic carriers from a large Brazilian pedigree of 11778 Leber hereditary optic neuropathy. Invest Ophthalmol Vis Sci 46:4809–4814
65. Ventura DF, Gualtieri M, Oliveria AGF, Costa MF, Quiros P, Sadun F, de Negri AM, Salomão SR, Berezovsky A, Sherman J, Sadun AA, Carelli V (2007) Male prevalence for acquired color vision defects in asymptomatic carriers of Leber's hereditary optic neuropathy. Invest Ophthalmol Vis Sci 39: 2362–2370